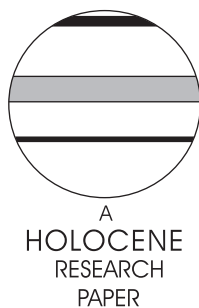


A 9111 year long conifer tree-ring chronology for the European Alps: a base for environmental and climatic investigations

K. Nicolussi,^{1*} M. Kaufmann,¹ Thomas M. Melvin,²
J. van der Plicht,³ P. Schießling¹ and A. Thurner¹

(¹Institute of Geography, University of Innsbruck, Innrain 52, 6020 Innsbruck, Austria; ²Climate Research Unit, Department of Environmental Sciences, University of East Anglia, Norwich NR4 7TJ, UK; ³Center for Isotope Research, Groningen University, Nijenborgh 4, 9747 AG Groningen, The Netherlands)

Received 2 July 2008; revised manuscript accepted 24 March 2009



Abstract: An ultra-long tree-ring width chronology (9111 years long, 7109 BC to AD 2002) has been established based on the analysis and dating of 1432 subfossil/dry dead wood samples and cores from 335 living trees. The material was collected from treeline or near-treeline sites (c. 2000 to 2400 m a.s.l.) mainly in the Eastern Alps. The availability of preserved samples through time at high altitudinal sites is influenced by Alpine forest history and is partly climatically controlled, as shown by comparisons of the sample depth record of the Eastern Alpine Conifer Chronology (EACC) with the Holocene glacier record. The similarity of variations over time between the sample depth of the chronology and the mid-Holocene GISP2 ¹⁰Be record suggest a relationship between sample depth and solar activity. The Eastern Alpine Conifer Chronology has already been used as a dating base in environmental studies, eg, on glacier fluctuations, as well as in archaeological studies.

Key words: Alps, Holocene, dendrochronology, radiocarbon dating, tree-ring chronology, *Pinus cembra*, *Larix decidua*, *Picea abies*, tree-line, solar activity.

Introduction

Knowledge of climatic variability in the past is an important basis for the validation of climate models and improvement to the assessment of the likelihood and analysis of the possible consequences of different scenarios of climatic change. The Alps, as a high mountain region, are particularly well suited for palaeoclimatic studies, because in this area evidence of climate variability has been preserved by variations in a number of environmental indicators, such as glaciers and the Subalpine treeline, whose relatively straightforward climate relationships allow them to be used as proxy climate data. Both the variations of the treeline and glacial advances have been used for the reconstruction of climatic history during the Holocene (eg, Patzelt and Bortenschlager, 1973; Furrer et al., 1987). Mountain glacier variations usually reflect longer-term climatic processes on timescales of decades to centuries. However, in most cases the time control for the recorded environmental and climatic events and changing conditions is limited by the temporal resolution of radiocarbon dating. Thus the

temporal synchrony of events dated at different sites or the duration of certain climatic conditions may be difficult to assess.

Compared with ¹⁴C-dated glacier and treeline records, dating and climatic reconstructions based on tree-ring studies have a much higher temporal resolution. The processes recorded by tree rings are exactly dated to a specific year and within the ring some seasonal events are recorded. By using sensitive tree species, climatic fluctuations of a short duration but high amplitude can be recorded and the accurate dating allows the establishment of regional and even hemispheric networks (eg, Briffa et al., 2002; Esper et al., 2002) to assess the impact of environmental events occurring in specific years (eg, Larsen et al., 2008). Moreover, tree-ring data from the Subalpine zone of the Alps allows the definition of a relatively clear relationship between climate variability and tree-ring growth. Summer temperature is the main factor determining tree-ring variability of high elevation sites at or near the treeline in the Alps (eg, Eckstein and Aniol, 1981; Schweingruber, 1987; Büntgen et al., 2005).

Dendrochronological studies on typical Alpine tree species, such as *Pinus cembra* and *Larix decidua* (Artmann, 1949; Brehme, 1951), were carried out a few years after the introduction

*Author for correspondence: (e-mail: Kurt.Nicolussi@uibk.ac.at)

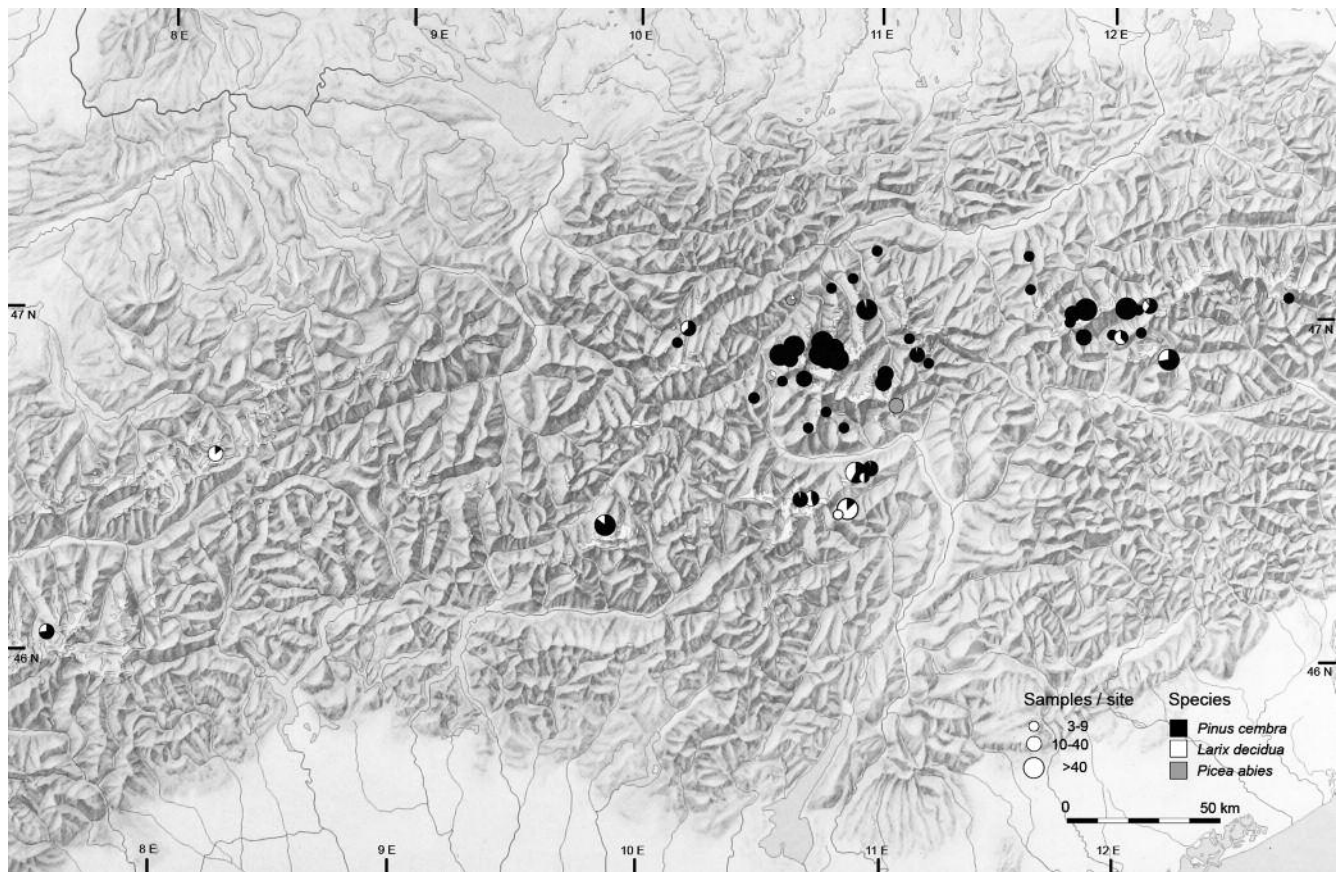


Figure 1 The sampling sites of the Eastern Alpine Conifer Chronology (sites > 2 samples only). Most of the sites are located in the western section of the central part of the Eastern Alps in Austria and Italy

of this science in central Europe by Huber (1941). These early investigations already demonstrated the potential of using these species to develop long chronologies. However, the establishment of a Holocene tree-ring chronology for the Alps has been missed until recent years. Up to the late 1990s, only the time period back to the early Middle Ages was covered by absolutely dated chronologies (eg, Donati *et al.*, 1988; Bebbler, 1990; Holzhauser, 1997; Nicolussi, 1999).

Efforts to establish a Holocene tree-ring chronology in the Alps, largely using wooden material from high elevation sites, were carried out in Switzerland in the 1970s and 1980s. R othlisberger *et al.* (1980), Bircher (1982), Renner (1982) and Sch ar and Schweingruber (1987, 1988) analysed subfossil samples from glacier forefields, peat bogs and small lakes. Mainly *Larix decidua* samples, together with some *Pinus cembra* and *Picea abies* samples were investigated. Based on this material it was possible to establish floating chronologies but not calendar-dated series (Kaiser, 1991). Further floating chronologies for different periods of the Holocene were established for the French Alps (Edouard *et al.*, 2002) and Austrian Alps (Grabner and Gindl, 2000; Nicolussi and Patzelt, 2000).

We present an absolutely dated tree-ring width chronology covering continuously 9111 years (7109 BC to AD 2002). It is the longest high mountain chronology in the world to date. The chronology is based on samples of the species *Pinus cembra* L., *Larix decidua* Mill. and *Picea abies* [L.] Karst., respectively, from high elevation sites in the European Alps. Moreover, the relevance of this chronology for studies on the Holocene environmental evolution and climatic fluctuations in the Alps is highlighted and discussed.

Material and methods

Fieldwork was carried out between 1998 and 2006. We mainly searched for subfossil logs at or near the surface of peat bogs (down to about 0.7 m) and in small lakes at high-altitude locations (usually between 2000 and 2400 m a.s.l.). This was done in the western section of the central Eastern Alps (Figure 1, Table 1) on both sides of the main Alpine ridge. At two sites (both in the Radurscheltal, Table 1) we also sampled a subset of 89 dry-dead logs that grew in the last millennium. From the subfossil and dry-dead logs, disc samples were taken for tree-ring analysis. In the central part of the Eastern Alps current treeline positions are located at about 2200 to 2400 m a.s.l. (Mayer, 1974). The high elevation forests in this area are dominated by *Pinus cembra* mixed with *Larix decidua* and, at lower elevations, *Picea abies*.

Subalpine *Pinus cembra* trees can live up to almost 800 years, but more common is a maximum lifespan of about 400 years. *Larix decidua* trees can reach similar life spans or even a little longer (Sch ar and Schweingruber, 1987, 1988). In contrast to this, only a few *Picea abies* trees have more than 300 tree rings. The number of rings available for analyses are usually less than the tree's lifespan because of the effects of decay processes.

In addition to the samples from peat bogs and small lakes, subfossil material of these tree species was collected on glacier forefields of the Austrian, Italian and Swiss Alps (eg, Nicolussi and Patzelt, 2000, 2001; J orin *et al.*, 2006, 2008; Nicolussi *et al.*, 2006). The locations of these samples showed a similar altitudinal range (about 1950 to 2200 m a.s.l.). The most recent time period is represented by tree-ring data derived from cores extracted from living trees (Nicolussi *et al.*, 1995) and discs taken from dry-dead logs (Lumassegger, 1996).

Table 1 The sampling sites of the Eastern Alpine Conifer Chronology (for dated samples > 2, state 2008)

Valley, local site	Site code	Coordinates	Aspect	Altitude (m a.s.l.)	Site type	Samples (<i>n</i>)
Ahrntal, Göge Alm	GGAA	11°49'E / 46°58'N	S	2195	p.bog	15
Ahrntal, Kofler Alm	KOFL	12°06'E / 46°57'N	S	2165–2190	p.bog	6
Ahrntal, Moaralm	AHMO	12°05'E / 47°02'N	SE	1995	p.bog	74
Ahrntal, Pojenalm 1	AHPJ	11°58'E / 46°57'N	SW	2020	p.bog	8
Ahrntal, Pojenalm 2	AHPO	11°59'E / 46°57'N	W	2040	p.bog	5
Ahrntal, Starklalm	AHST	12°07'E / 47°03'N	S	2080	p.bog	10
Ahrntal, Waldner Alm	AHWA	12°06'E / 47°03'N	SE	2100	p.bog	4
Defereggental, Hirschbichl	HIB	12°15'E / 46°54'N	E	2140	lake/p.bog	47
Haslital, Unteraargletscher	UA	8°13'E / 46°34'N	E	1950	glacier f.	28
Kaunertal, Daunmoränensee	GDM	10°43'E / 46°53'N	E	2295	lake/p.bog	49
Kaunertal, Gepatschferner	GP	10°44'E / 46°52'N	W	2060–2275	glacier f.	44
Kaunertal, Krummgampen	KG	10°42'E / 46°52'N	E	2385–2410	p.bog	25
Kaunertal, Ochsenalm	KOA	10°43'E / 46°53'N	SE	2160–2190	p.bog	44
Kaunertal, Ombrometer	GLI	10°43'E / 46°53'N	NE	2135–2160	p.bog	44
Kühtai, Wörgetal	WTL	10°58'E / 47°13'N	N	1985	lake	6
Langtaufers, Pedrosbach	LPE	10°34'E / 46°49'N	SE	2400–2510	p.bog	5
Langtaufers, Sandbichl	LFS	10°42'E / 46°49'N	NW	2330–2340	p.bog	14
Martelltal, Zufallhütte (A-D)	ZUFA-D	10°41'E / 46°28'N	N	2200–2300	p.bog	20
Martelltal, Zufallhütte (E-R)	ZUFE-R	10°41'E / 46°29'N	SE	2140	p.bog	11
Matschertal, Upital	MAT	10°42'E / 46°42'N	W	2400	p.bog	3
Mölltal, Pasterze	PAZ	12°45'E / 47°04'N	SE	2070	glacier f.	3
Montafon, Klostertal	SIKL	10°04'E / 46°53'N	SE	2125–2200	p.bog	4
Navistal, Klammalm	KLA	11°36'E / 47°09'N	W	2130	p.bog	3
Oberes Gericht, Komperdellalm	KPD	10°34'E / 47°02'N	SE	1940	p.bog	5
Ötztal, Ebenalm	EBA	10°57'E / 47°01'N	NE	2060–2170	lake/p.bog	76
Ötztal, Gurgler Alm	GGUA	11°00'E / 46°51'N	W	2150–2200	p.bog	23
Ötztal, Gurgler Zirbenwald	G/SMG/GX	11°01'E / 46°51'N	NW	2060	p.bog	33
Ötztal, Krottenlacke	KRO	11°06'E / 46°57'N	SW	2280	lake	3
Ötztal, Leierstal	LEI	10°51'E / 47°42'N	N	2885	p.bog	4
Passeier, Schneeberg-Seemoos	SMO	11°10'E / 46°53'N	SW	2140	p.bog	3
Passeier, Timmeltal	TAH	11°08'E / 46°54'N	S	1975–2260	p.bog	29
Paznaun, Bielerhöhe	BIH	10°06'E / 46°55'N	N	1930–2020	p.bog	11
Pffelderer Tal, Lazinsalm	LAZA	11°04'E / 46°47'N	NE	1770	debris	15
Pitztal, Brechsee	BRS	10°47'E / 47°05'N	N	2145	lake	9
Radurscheltal, Berglboden	BER	10°36'E / 46°54'N	N	2250–2300	surface	10
Radurscheltal, Miseri	MIS	10°37'E / 46°54'N	N	2205–2300	surface	79
Radurscheltal, Sattelalm	RSA	10°34'E / 46°55'N	NE	2060–2070	p.bog	49
Schnalstal, Lazaunsee	LZS	10°45'E / 46°45'N	E	2425–2430	lake/p.bog	8
Schnalstal, Penaudalm	SPA	10°54'E / 46°41'N	E	2310–2395	p.bog	6
Ultental, Fiechtsee	ULFI	10°50'E / 46°28'N	N	2110	lake/p.bog	94
Ultental, Weißbrunnalm	UWBA	10°49'E / 46°28'N	NE	2330	p.bog	3
Val d'Herens, Glacier du Mont Miné	MM	7°55'E / 46°01'N	NNE	2150	glacier f.	26
Val Roseg, Vadret da Tschierva	TSC	9°53'E / 46°24'N	NW	2115–2210	glacier f.	41
Vinschgau, Marzoneralm (A)	MAZA	10°58'E / 46°35'N	N	2225	lake/p.bog	10
Vinschgau, Marzoneralm (B-F)	MAZB-E	10°57'E / 46°35'N	N	2105–2145	p.bog	150
Vinschgau, Plamourt	REPL	10°49'E / 46°28'N	NW	2040	p.bog	6
Vinschgau, Rojental	RT	10°28'E / 46°48'N	SE	2400	p.bog	3
Vinschgau, Zirmtalsee	ZTS	10°58'E / 46°35'N	N	2115–2120	lake/p.bog	26
Wattental, Möslalm	WLI	11°35'E / 47°10'N	NW	2200	p.bog	3
Zillertal, Gh. Alpenrose	ZAR	11°48'E / 47°01'N	SE	1875–1880	p.bog	12
Zillertal, Goldboden	UGB	11°47'E / 47°01'N	N	2120–2150	p.bog	3
Zillertal, Schwarzensteinmoor	SSM	11°49'E / 47°01'N	SE	2120–2160	p.bog	184
Several sites (samples a site < 3)	–	–	–	–	glacier f./ lake/ p.bog	36

All samples are subfossil with the exception of those from the sites Radurscheltal-Miseri and Radurscheltal-Berglboden (sample code MIS and BER). Site type: glacier f., glacier forefield; p.bog, peat bog.

Measurements were made of the total tree-ring width and these were recorded to the nearest 0.001 or 0.005 mm. A minimum of two radii from each tree were analysed and a tree-ring series for each tree was established by synchronizing and averaging the measurements of all radii (precision 0.001 mm) for that tree. These 'mean tree' sample series were used in comparisons with other tree-ring series and reference chronologies. We used visual and statistical comparisons between single series and already established chronologies to find the exact crossdating position for each single tree-ring series. Visual and statistical comparisons were performed after high-pass filtering of the original measurement series. We applied a 30 yr spline (Cook and Peters, 1981) to remove age-related growth trends from the series.

Additionally, radiocarbon dating was applied extensively mainly at the beginning of chronology building to establish in a first step a framework of approximately dated tree-ring series and chronologies (Nicolussi *et al.*, 2004). In the latter phases of the project radiocarbon dating was mainly used on samples without satisfactory crossdating results. All wood material used for radiocarbon dating was taken after initial dendrochronological analysis of the disc and in each case the precise position from within the sequence of tree-rings was recorded. Table 2 lists the radiocarbon dates established and the position of the radiocarbon sample within the tree-ring series. Conventional radiocarbon dating was used for the majority of the samples. Radiocarbon dating of multiple samples of material, from known relative positions within a dated dendrochronological sequence, allowed the application of wiggle matching as an advanced radiocarbon dating technique. The calibration of ^{14}C -dates (Table 2) including wiggle matching was performed using OxCal 3.1 (Bronk Ramsey, 2001) and the IntCal04 calibration data set (Reimer *et al.*, 2004). OxCal 3.1 uses a Bayesian approach for wiggle matching calculations (Bronk Ramsey, 1995; Bronk Ramsey *et al.*, 2001). As well as conventional radiocarbon dating, a sequence of decadal AMS ^{14}C -dates utilizing dendrochronologically dated samples from this tree-ring chronology project was established for the time period 3500 to 3000 BC (for data and results see Dellinger *et al.*, 2004).

A 30 yr high-pass filter was applied to the individual tree-ring series used for the establishment of the chronology (Figure 2). Chronology strength has been assessed by the calculation of the mean interseries correlation (RBAR, Figure 2) and the 'expressed population signal' (EPS, Wigley *et al.*, 1984) values. RBAR and EPS results were calculated using a 50 yr window with a 25 yr overlap of the windows. There can be problems with the calculation of RBAR and EPS when using multiple cores from individual trees as shown by Esper *et al.* (2006) because of the marked difference between within-tree and between-tree correlations. Here these problems were avoided by using mean-tree and mean-sample series and thus excluding within-tree correlations which would probably result in generally higher EPS numbers (D'Arrigo *et al.*, 2001). The chronology presented (Figure 2) is also based on mean-tree and mean-sample series.

The Eastern Alpine Conifer Chronology

The Eastern Alpine Conifer Chronology (EACC) established here covers 9111 years (from 7109 BC to AD 2002). This is presently the longest chronology from a mountainous area worldwide. In Europe it is the most southerly located ultra-long tree-ring chronology. Most samples are from sites in the western part of the Eastern Alps (Figure 1). The EACC is based on 1343 subfossil and 89 dry-dead samples, respectively, and cores from 335 living trees (only *Pinus cembra*). The non-recent part of the chronology

(subfossil and dry-dead material) is clearly dominated by samples of *Pinus cembra* ($n=1167$, 81.5%), with *Larix decidua* ($n=237$, 16.6%) and *Picea abies* ($n=28$, 1.9%) as minor fractions. The majority of the *Picea abies* samples originate from a single site at relatively low altitude (site Lazins, Table 1, Figure 1: the only complete grey point). The *Larix decidua* samples are mainly from sites south of the main Alpine ridge and from glacier forefields (Figure 1). This distribution is consistent with recent environmental conditions that show extensive larch forests in the treeline ecotone in the southern part of the Alps while current treeline forests north of the main Alpine ridge usually consists of pure *Pinus cembra* trees. Larch trees also prefer the open conditions in glacier forefields and usually dominate forests at such sites at least in initial stages of forest establishment. *Pinus cembra* tree-ring series occur throughout the entire length of the Alpine chronology whereas the coverage by larch samples extends from 6981 BC to AD 1976 and has gaps from 3363 to 3311 BC, 4471 to 4227 BC and 6184 to 6111 BC (Figure 3).

The error ranges of the conventional radiocarbon results (Table 2) of the samples analysed largely encompass or overlap partly (94% of the samples, Table 2) the dendrochronologically established calendar dates of the tree-ring sequences, thus confirming the results by Dellinger *et al.* (2004) who used a set of 50 decadal samples and ^{14}C -dates covering the time period 3500 to 3000 BC. In general this perfect fit between dendrochronological dates and ^{14}C -results is also true for the radiocarbon samples older than about 6100 BC. Figure 4 shows these radiocarbon dates in relation to the IntCal04 calibration curve (Reimer *et al.*, 2004). A comparison of the dendro-dates of the radiocarbon-dated wood material with the calibrated ^{14}C -results shows two outliers (Table 2, samples TAH-6 and SSM-106) in the millennium between 7100 and 6100 BC. The reason why these two are anomalous is not clear, and will be further investigated. If the two outliers are not considered the 'wiggle matching' of the other 13 radiocarbon dates before 6100 BC fits nearly perfectly the expected results from tree-ring dating. The mean values of the 2σ range of the ^{14}C calibration differ only by approximately one year from the central value of the dendrochronologically established dating of the ^{14}C -dated tree-ring sequences (Figure 4). There are several potential causes for outliers, eg, errors in sample extraction. However, Dellinger *et al.* (2004) could also show that in some time periods statistically significant differences can occur between the ^{14}C content of Alpine samples in relation to the reference data. Such effects could also explain some outliers of the radiocarbon dates (Table 2).

The tree-ring series used for the EACC are not equally distributed over the whole length of the chronology (Figure 3). The sample depth shows a generally negative trend by increasing age. Maximum replication falls into the last millennium when also 89 dry-dead samples with a mean segment length of 308.9 years are included in the chronology. In general the last two millennia show the highest number of samples per year, which can be explained by variation in the conditions required to preserve samples, the proximity to the surface of subfossil logs and the possibility to find dry-dead trees. The number of samples drops below ten only three times during the last 9000 years: around 350 BC, 1100 BC and 6100 BC. The latter period has the minimum sample density ($n=4$) of the whole chronology.

Though individual tree ages of 400 to 1000 years can be reached by the tree species used here there is a tendency for only the trees that grow slowly to become very old and the additional requirement that the tree must be growing in a situation where it can be preserved. The mean segment length of the subfossil/dry-dead samples is only 209.9 tree rings. Larch series show a higher mean segment length (248 tree rings) than the *Pinus cembra* (202.5 tree rings) and the *Picea abies* samples (197 tree rings), respectively. The relatively low segment length in relation to the

potential lifespan of the trees is probably caused by different factors. Decay processes are primarily responsible eg, easily recognizable by missing inner parts of logs or missing sapwood. Some trees grew in environments, eg, glacier forefields, where lifetime can be limited by glacier advances. Some of the sites investigated are located within the Holocene treeline ecotone, where climatic fluctuations can also limit the lifetime of trees.

RBAR and EPS calculations illustrate generally fluctuating results around the average of 0.26 and 0.89, respectively (Figure 2). Only the time period between approximately 5400 and 4850 BC shows continuously low RBAR values synchronous with lowest variability of the tree-ring width data. This and the relatively low sample depth of the EACC at that time result in an EPS value (Wigley *et al.*, 1984) that passes the commonly used 0.85 threshold for a satisfactory chronology signal (Figure 2).

The other periods of EPS values below the 0.85 threshold, eg, around 8100 BC, 1200 BC and 300 BC, are mainly caused by low replication (Figures 2 and 3). However, for most sections of the EACC, EPS values are above the commonly used threshold of 0.85. The chronology strength measured by RBAR and EPS is of the high-frequency common signal and larger numbers of samples and also different standardization techniques will be needed to extract the long-timescale variation of climate from this chronology.

Discussion

Our efforts during recent years have successfully established the first ultra-long Alpine tree-ring chronology. However, a number of chronologies or single tree-ring series had previously been derived from subfossil wooden samples from high elevation sites in the Alps since the 1970s (eg, Röthlisberger *et al.*, 1980; Bircher, 1982; Renner, 1982; Schär and Schweingruber, 1987, 1988; Holzhauser, 1997; Edouard *et al.*, 2002; Grabner *et al.*, 2001). These chronologies and series were originally only ^{14}C dated. However, using the EACC as a dating base the establishment of exact calendar dates for most of these series was successful. Figure 5 displays the EACC and the other synchronized conifer series and chronologies. Note, there is no data overlap between the EACC series and the other series and chronologies shown in Figure 5 (eg, from Höhenbiel) with the exception of some archaeological samples ($n=13$). As a result, there is now an Alpine network of absolutely dated chronologies covering the last 9100 years and nearly the whole range of the high-altitude Alps.

It is highly significant that there is a common high-frequency signal in the growth of samples from near-treeline sites across a wide area including the Swiss (eg, Höhenbiel: Bircher, 1982; Renner, 1982) and even French Alps (Edouard *et al.*, 2002). However, series from sites at lower elevations (eg, Grächen, Schweingruber and Schär, 1987, 1988) do not always show satisfying synchronization results. The vertical distance to the local species-specific treeline is a better predictor of the potential for crossdating than the absolute altitude, because the amplitude of the common signal in tree growth caused by variation in temperature is larger for trees which are closer to their species specific low-temperature limit and the absolute value of temperature varies with altitude. For example, the synchronization of *Picea abies* samples from the Schwarzensee (Dachstein region, Austria; Grabner and Gindl, 2000; Grabner *et al.*, 2001) with the EACC was usually successful because this species is near its altitudinal limit but crossdating of *Pinus cembra* series from trees growing at the same site, which is well below the elevation of the *Pinus cembra* treeline in this region, often failed.

The EACC has already been used as a dating base for studies of environmental changes in the Alps. Important results were achieved

in the field of Holocene glacier history. Several Neoglacial advances of the glacier Gepatschferner, Eastern Alps, were established by the analysis and dating of overridden trees (Nicolussi and Patzelt, 2001; Nicolussi *et al.*, 2006). Tree-ring chronologies of the first millennium BC and AD, respectively, from the Great Aletsch glacier, Swiss Alps, based on logs from the so-called Göschenen I and Göschenen II advance periods (Holzhauser, 1997), were also synchronized and therefore calendrically dated with the EACC (Holzhauser *et al.*, 2005). A record of the evolution of the Alpine treeline during the Holocene was established by tree-ring dating of logs and wooden remains found at sites above the current treeline position (Nicolussi *et al.*, 2005). The EACC has also been used successfully as a dating base for archaeological samples. However, this field of application of the EACC is limited to samples from high elevation sites, eg, the log boat from the Obersee, Austria (Reitmaier and Nicolussi, 2002), mining timbers from Bronze age copper mining at the Kelchalm, Austria (Pichler *et al.*, 2009) and the Bronze Age wooden construction for tapping a spring in St Moritz, Switzerland (Seifert, 2000; Nicolussi *et al.*, 2004). Tree-ring series from Alpine treeline and near-treeline sites, respectively, are generally suited for (summer) temperature reconstructions (eg, Eckstein and Aniol, 1981; Nicolussi, 1995; Büntgen *et al.*, 2005). This has also been demonstrated by using the *Pinus cembra* samples of the most recent part of the EACC in a summer temperature reconstruction for the past millennium (Büntgen *et al.*, 2005). Major climatic events of the Northern Hemisphere, eg, following the Tambora 1815 eruption, trigger a tree growth response which is clearly visible in the EACC. The major climatic disturbances *c.* AD 540, presumed to be the results of major volcanic eruptions, caused a marked reduction of tree growth in the Alps as has been demonstrated by Larsen *et al.* (2008), who included the *Pinus cembra* and *Larix decidua* data of the last 2000 years from the EACC in a Eurasian network of tree-ring chronologies. Synchronous climatic effects in wide areas of Europe and Asia resulting from these events were identified by this study (Larsen *et al.*, 2008).

A critical point of any tree-ring chronology is sample replication. It influences both dating ability and the potential use of the chronology for dendroclimatic reconstructions. The number of tree-ring series in each year of the EACC fluctuates remarkably on an interannual to centennial scale (Figure 3). Variability in the sample depth of multimillennial records has been recognized as controlled by climatic but also non-climatic causes (eg, Naurzbaev *et al.*, 2002; Spurk *et al.*, 2002). The reasons for the fluctuating replication of the EACC are likely a combination of search strategies for samples, climatic and anthropogenic impacts on the Subalpine forests in the past, variation in the conditions required for preservation and even coincidence. The general decrease of sample depth with increasing age is most probably an effect of the sampling approach, eg, the concentration of the uppermost approximately 0.7 m in peat bogs. The high number of samples from the last millennium can largely be attributed to dry-dead samples lying on the surface. However, surface wood from earlier millennia is unlikely to have survived. The periods of low sample depth during the first two millennia BC could be caused by both climatic and anthropogenic impact. During these periods several glacier advances occurred and Alpine treelines declined sharply (Patzelt and Bortenschlager, 1973; Wick and Tinner, 1997; Nicolussi and Patzelt, 2001). Both records indicate cooler climatic conditions and, in addition to lower treelines, forest density within the treeline ecotone can be expected to be reduced. Therefore the potential to find wooden remains from those periods at high altitude sites is reduced. Moreover, pollen analyses and radiocarbon dating of charcoal layers show that human impact on the treeline ecotone of the Eastern Alps increased in the Bronze Age (2200 to 800 BC) and Iron Age (800 to 15 BC) (Patzelt, 1996; Bortenschlager, 2000).

Table 2 The conventional ^{14}C -dates of samples used for the establishment of the Eastern Alpine Conifer Chronology (LADE, *Larix decidua*; PCAB, *Picea abies*; PICE, *Pinus cembra*)

Sample code	Species	Mean segment length (n)	^{14}C sample (tree-ring series no.)	Laboratory code	^{14}C -age (yr BP)	Cal. ^{14}C -age (1σ) (yr BC/AD)	Cal. ^{14}C -age (2σ) (yr BC/AD)	Absolute age of the tree-ring series (yr BC/AD]
BIH-3	LADE	166	62–87	GrN-28696	4090±30	2840–2570 BC	2860–2490 BC	2646–2481 BC
BIH-7	PICE	300	137–152	GrN-28697	8015±40	7060–6830 BC	7070–6770 BC	7109–6810 BC
BIH-11	LADE	212	45–61	GrN-28698	7035±40	5985–5890 BC	6010–5830 BC	6029–5818 BC
FAA-1	PICE	122	57–69	GrN-29531	5330±35	4240–4060 BC	4320–4040 BC	4257–4136 BC
FPGG-1	LADE	387	298–313	GrN-29532	360±15	1470–1620 AD	1450–1630 AD	1194–1580 AD
G-1	PICE	405	1–31	Hd 16850	1808±24	130–250 AD	130–320 AD	224–628 AD
G-2	PICE	509	1–10	Hd 12896	1855±30	125–220 AD	80–240 AD	159–667 AD
G-17	PICE	315	73–92	Hd 16849	1472±19	565–615 AD	550–640 AD	546–888 AD
G-25	PICE	292	19–43	Hd-17701	1377±15	645–660 AD	635–670 AD	625–916 AD
G-26	PICE	215	11–26	Hd-16518	1078±26	890–1020 AD	890–1020 AD	894–1108 AD
G-29	PICE	225	1–12	Hd-12631	1400±40	610–660 AD	570–680 AD	659–883 AD
G-35	PICE	206	22–36	GrN-10056	1885±40	60–210 AD	20–240 AD	130–335 AD
GDM-1	PICE	334	9–21	GrN-21551	7650±40	6560–6440 BC	6600–6440 BC	6483–6150 BC
GDM-1B	PICE	334	133–163	GrN-27061	7490±30	6430–6270 BC	6440–6250 BC	6483–6150 BC
GDM-3	PICE	339	22–41	Hd-17700	5838±24	4770–4680 BC	4790–4610 BC	4703–4366 BC
GDM-4	PICE	309	9–30	GrN-21549	5990±25	4935–4835 BC	4950–4790 BC	4920–4611 BC
GDM-7	PICE	136	47–71	GrN-24824	7720±35	6595–6505 BC	6640–6470 BC	6634–6499 BC
GDM-8	PICE	261	16–26	GrN-24825	4940±20	3760–3660 BC	3770–3650 BC	3939–3679 BC
GDM-11	PICE	445	14–29	GrN-24826	6945±30	5880–5770 BC	5900–5730 BC	5886–5432 BC
GDM-12	PICE	290	82–128	GrN-24827	4335±20	3010–2900 BC	3020–2900 BC	3215–2926 BC
GDM-14	PICE	215	14–40	GrN-24828	7085±35	6010–5915 BC	6030–5890 BC	6011–5797 BC
GDM-18	PICE	288	215–243	GrN-24829	4125±30	2860–2620 BC	2870–2570 BC	3035–2747 BC
GDM-21	PICE	150	6–33	GrN-24830	7215±35	6100–6015 BC	6210–6000 BC	6171–6022 BC
GDM-25	PICE	178	36–49	GrN-24831	4990±30	3795–3710 BC	3940–3690 BC	3800–3622 BC
GDM-30	PICE	509	333–349	GrN-24832	3760±20	2205–2140 BC	2280–2050 BC	2625–2117 BC
GDM-31	PICE	273	45–74	GrN-24833	5200±20	4040–3970 BC	4045–3965 BC	4097–3827 BC
GDM-32	PICE	254	24–44	GrN-24834	4050±25	2620–2490 BC	2840–2480 BC	2665–2412 BC
GDM-34	PICE	169	22–28	GrN-24835	4955±20	3770–3700 BC	3790–3660 BC	3904–3736 BC
GDM-38	PICE	357	252–264	GrN-24836	4200±20	2890–2760 BC	2890–2690 BC	3155–2799 BC
GLI-44	PICE	165	10–21	GrN-25667	6180±30	5210–5070 BC	5220–5030 BC	5107–4943 BC
GLI-45	PICE	234	135–170	GrN-27732	2505±30	770–550 BC	790–520 BC	713–480 BC
GP-20	PICE	276	1–17	Hd-14043	1930±20	30–120 AD	20–130 AD	53–328 AD
GP-21	PICE	87	47–65	GrN-22579	1815±35	130–240 AD	80–230 AD	244–330 AD
GP-22	PICE	236	45–66	GrN-22580	2810±40	1010–910 BC	1090–840 BC	952–717 BC
GP-23	PICE	104	78–89	GrN-21937	2440±25	730–410 BC	750–400 BC	741–638 BC
GP-25	PICE	152	33–52	GrN-24726	940±20	1030–1160 AD	1020–1160 AD	1063–1214 AD
GP-26	PICE	195	109–124	Hd-15286	976±15	1020–1120 AD	1010–1150 AD	933–1127 AD
GP-63	PICE	90	50–63	GrN-22582	2490±35	770–540 BC	780–410 BC	808–719 BC
GP-64	PICE	125	100–110	Hd-15472	2432±16	540–410 BC	740–400 BC	762–638 BC
GP-65	PICE	149	1–20	Hd-15666	3445±23	1870–1690 BC	1880–1680 BC	1781–1633 BC
GP-80	PICE	109	66–89	Hv-11411	3420±70	1880–1620 BC	1900–1520 BC	1753–1645 BC
GP-96	PICE	204	65–100	GrN-27062	3710±20	2140–2040 BC	2200–2030 BC	2190–1987 BC
GP-104	PICE	239	59–75	GrN-22766	3350±30	1690–1600 BC	1740–1530 BC	1796–1558 BC
GP-106	PICE	240	86–122	GrN-22767	6610±40	5620–5510 BC	5620–5480 BC	5617–5378 BC
GP-107	PICE	142	38–50	GrN-23632	1371±17	645–665 AD	640–675 AD	616–757 AD
GP-129	PICE	96	66–85	GrN-24730	2495±25	760–540 BC	780–520 BC	734–639 BC
GP-60100	PICE	166	33–57	GrN-22581	1925±35	30–130 AD	40 BC–210 AD	2 BC–164 AD
KG-6	PICE	197	7–26	GrN-24542	6205±25	5220–5070 BC	5290–5050 BC	5125–4929 BC
KG-7	PICE	298	208–219	GrN-24543	5680±30	4545–4460 BC	4600–4450 BC	4674–4377 BC
KG-8	PICE	174	39–49	GrN-24544	7125±25	6025–5985 BC	6060–5920 BC	6036–5863 BC
KG-11	PICE	374	235–257	GrN-24733	7910±30	6830–6685 BC	7030–6650 BC	7090–6717 BC
KG-13	PICE	158	149–155	GrN-25213	6200±35	5220–5070 BC	5300–5040 BC	5247–5090 BC
KG-17	PICE	346	36–43	GrN-25214	6400±30	5470–5320 BC	5470–5320 BC	5401–5056 BC
KG-19	PICE	120	101–119	GrN-28700	6420±35	5470–5360 BC	5480–5320 BC	5497–5378 BC
KOA-1	PICE	192	123–164	GrN-24734	4690±30	3520–3370 BC	3630–3370 BC	3567–3376 BC
KOA-2	PICE	191	60–88	GrN-24735	4360±30	3015–2915 BC	3090–2900 BC	3046–2855 BC
KOA-5	PICE	307	30–46	GrN-24736	3580±25	1955–1890 BC	2030–1880 BC	2047–1741 BC
KOA-7	PICE	211	115–139	GrN-24837	3310±20	1620–1530 BC	1640–1520 BC	1851–1641 BC
KOA-10	PICE	175	44–60	GrN 25668	7420±50	6370–6230 BC	6430–6210 BC	6405–6231 BC
KOA-57	PICE	169	94–107	GrN-28702	4500±30	3340–3100 BC	3350–3090 BC	3240–3072 BC
KPD-1	PCAB	231	21–50	GrN-25318	2975±20	1270–1130 BC	1300–1120 BC	1214–984 BC
KPD-6	PCAB	370	192–208	GrN-23746	6435±25	5470–5375 BC	5480–5340 BC	5574–5205 BC
KPD-7	LADE	213	48–70	GrN-25321	3630±20	2025–1960 BC	2120–1920 BC	1980–1768 BC
KPD-9	PCAB	338	168–193	GrN-23747	4450±30	3320–3020 BC	3340–2960 BC	3455–3118 BC

Table 2 (Continued)

Sample code	Species	Mean segment length (<i>n</i>)	¹⁴ C sample (tree-ring series no.)	Laboratory code	¹⁴ C-age (yr BP)	Cal. ¹⁴ C-age (1 σ) (yr BC/AD)	Cal. ¹⁴ C-age (2 σ) (yr BC/AD)	Absolute age of the tree-ring series (yr BC/AD)
KRO-1	PICE	183	30–46	GrN-22583	7090±50	6020–5910 BC	6060–5870 BC	6002–5820 BC
KRO-2	PICE	118	23–42	GrN-24545	4665±20	3510–3370 BC	3520–3360 BC	3509–3392 BC
KRO-3	PICE	258	7–45	GrN-24546	6730±40	5705–5615 BC	5720–5560 BC	5665–5408 BC
LPE-11	PICE	74	25–50	GrN-26122	6040±30	5000–4850 BC	5020–4840 BC	4933–4860 BC
LPE-14	PICE	150	43–56	GrN-26123	5400±25	4325–4240 BC	4340–4170 BC	4148–3999 BC
LPE-15	PICE	291	81–120	GrN-26124	5410±30	4330–4255 BC	4340–4170 BC	4329–4039 BC
LZS-2	PICE	244	17–27	GrN-25215	5280±25	4230–4040 BC	4230–3990 BC	4126–3883 BC
LZS-6	PICE	153	109–125	GrN-25322	200±20	1660–1960 AD	1650–1960 AD	1701–1853 AD
LZS-7	PICE	128	101–115	GrN-25323	7600±50	6485–6410 BC	6570–6380 BC	6575–6448 BC
LZS-9	PICE	115	8–22	GrN-25324	7760±30	6640–6530 BC	6650–6500 BC	6607–6493 BC
LZS-10	PICE	96	35–47	GrN-25325	2085±25	160–50 BC	180–40 BC	142–47 BC
PAZ-24	PICE	128	75–99	Hd-17687	5066±20	3950–3800 BC	3950–3790 BC	3906–3779 BC
PAZ-32	PICE	76	1–14	GrN-23776	5995±25	4935–4840 BC	4950–4790 BC	4861–4786 BC
PAZ-40	PICE	164	105–164	GrN-25195	4100±20	2840–2580 BC	2860–2570 BC	2750–2587 BC
SKR-1	PICE	250	106–123	GrN-25217	6390±30	5470–5320 BC	5470–5310 BC	5571–5322 BC
SMO-3	PICE	250	150–168	GrN-25669	6100±30	5055–4960 BC	5210–4930 BC	5231–4982 BC
SPA-9	PICE	142	13–35	GrN-26129	6290±50	5315–5220 BC	5380–5070 BC	5179–5038 BC
SSM-1	PICE	124	60–65	GrN-25269	7980±40	7040–6820 BC	7050–6700 BC	7038–6915 BC
SSM-3	PICE	188	53–59	GrN-25270	3600±20	2010–1920 BC	2030–1890 BC	1972–1784 BC
SSM-7	PICE	71	35–49	GrN-29533	2835±20	1015–935 BC	1050–920 BC	1066–995 BC
SSM-20	PICE	146	138–143	GrN-25271	2045±20	90 BC–1 AD	160 BC–20 AD	230–85 BC
SSM-32	PICE	175	42–50	GrN-25272	5640±20	4495–4450 BC	4540–4390 BC	4515–4341 BC
SSM-48	PICE	205	62–67	GrN-25273	2205±25	360–200 BC	370–190 BC	372–168 BC
SSM-55	PICE	100	76–91	GrN-29534	3475±25	1880–1740 BC	1890–1690 BC	1926–1827 BC
SSM-57	PICE	107	37–56	GrN-26455	1350±25	650–680 AD	640–770 AD	637–743 AD
SSM-59	PICE	169	21–40	GrN-25274	4340±30	3010–2900 BC	3030–2890 BC	2972–2804 BC
SSM-66	PICE	207	32–41	GrN-25275	5165±20	3985–3955 BC	4040–3950 BC	4064–3858 BC
SSM-68	PICE	163	37–49	GrN-25276	5290±20	4230–4040 BC	4230–4040 BC	4252–4090 BC
SSM-71	PICE	171	16–68	GrN-25277	6030±30	4990–4850 BC	5010–4830 BC	4961–4791 BC
SSM-76	PICE	128	49–83	GrN-25278	4450±30	3320–3020 BC	3340–2960 BC	3076–2949 BC
SSM-79	PICE	197	23–33	GrN-25279	5320±25	4240–4060 BC	4240–4050 BC	4206–4010 BC
SSM-80	PICE	108	70–89	GrN-26456	4820±25	3650–3530 BC	3660–3520 BC	3705–3597 BC
SSM-85	PICE	181	23–38	GrN-25281	3890±25	2460–2340 BC	2470–2290 BC	2390–2210 BC
SSM-93	PICE	147	58–73	GrN-25282	3480±20	1880–1750 BC	1880–1740 BC	1871–1725 BC
SSM-94	PICE	158	37–44	GrN-25283	2460±20	815–795 BC	830–790 BC	736–579 BC
SSM-106	PICE	141	56–101	GrN-29535	7260±30	6210–6060 BC	6220–6050 BC	6395–6255 BC
SSM-218	PICE	120	32–68	GrN-28704	4960±35	3780–3695 BC	3900–3650 BC	3833–3714 BC
SSM-233	PICE	347	142–185	GrN-28705	7470±40	6400–6250 BC	6430–6240 BC	6440–6089 BC
SSM-235	PICE	127	81–104	GrN-28706	4850±35	3700–3540 BC	3710–3530 BC	3652–3526 BC
SSM-412	PICE	131	27–46	GrN-28707	5805±35	4715–4610 BC	4770–4540 BC	4746–4616 BC
SSM-414	PICE	76	28–44	GrN-28708	6865±40	5795–5705 BC	5840–5660 BC	5766–5691 BC
SSM-418	PICE	48	27–38	GrN-29538	5770±40	4690–4550 BC	4720–4520 BC	4663–4616 BC
TAH-1	PICE	168	5–14	GrN-24929	7405±35	6360–6230 BC	6390–6220 BC	6387–6220 BC
TAH-6	PICE	189	28–53	GrN-24838	7485±25	6420–6260 BC	6430–6250 BC	6519–6310 BC
TAH-7	LADE	260	8–27	GrN-24738	7930±35	7020–6690 BC	7030–6680 BC	6981–6722 BC
TAH-9	PICE	129	14–37	GrN-24930	7040±30	5985–5895 BC	6000–5840 BC	5880–5753 BC
TAH-20	PICE	159	19–32	GrN-27073	5720±25	4600–4515 BC	4690–4480 BC	4559–4401 BC
TSC-133	PICE	73	32–71	GrN-29540	5975±25	4910–4800 BC	4940–4790 BC	4909–4864 BC
TSC-136	PICE	102	92–101	GrN-29541	5025±30	3940–3760 BC	3950–3710 BC	3824–2723 BC
TSC-146	PICE	89	46–61	GrN-29542	5965±35	4900–4790 BC	4950–4720 BC	4899–4811 BC
TSC-148	PICE	289	169–262	GrN-29543	6155±35	5210–5040 BC	5220–5000 BC	5384–5096 BC
TSC-157	PICE	625	488–500	GrN-29544	6135±25	5210–5000 BC	5210–4990 BC	5495–4871 BC
UA-210	LADE	134	78–89	GrN-30656	2965±25	1260–1120 BC	1300–1110 BC	1352–1219 BC

Between about 5300 and 1700 BC the sample replication of the chronology shows minor fluctuations around a more or less constant long-term mean. The most pronounced minima, around 3700/3300 BC and around 4300 BC, are also known as periods of glacier advances in the Eastern Alps (Renner, 1982; Nicolussi and Patzelt, 2001). Additionally, the periods of higher replication in the middle Holocene correspond with known high treeline positions in the Alps (Wick and Tinner, 1997; Nicolussi *et al.*, 2005).

The lowest replication of the chronology is recorded around 6100 BC (Figure 3) and it is therefore synchronous with the prominent 8.2 ka event (von Grafenstein *et al.*, 1999; Alley and Agustsdottir, 2005). A decline of the treeline in the central Eastern Alps was shown for that time period, although its altitude did not fall below the level reached in the ‘Little Ice Age’ (Nicolussi *et al.*, 2005). The 8.2 ka event was the last of three pronounced climatic fluctuations during the early Holocene recorded in the Greenland

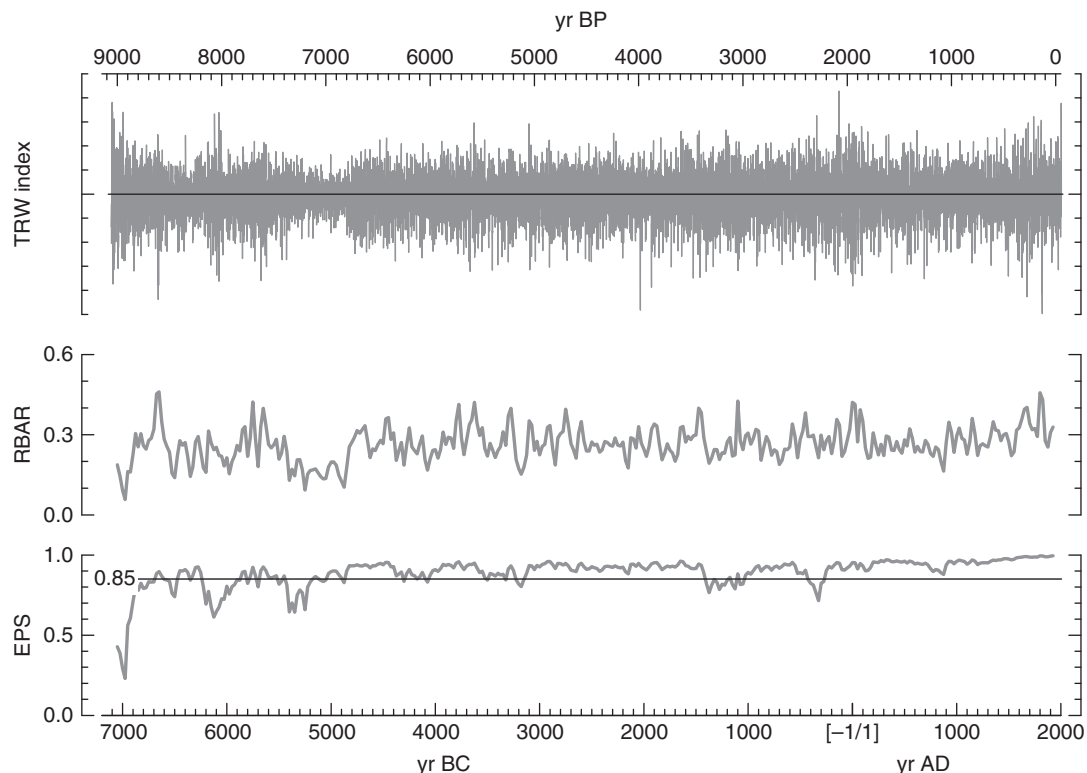


Figure 2 The Eastern Alpine Conifer Chronology (EACC). Upper panel: tree-ring width chronology after high-pass filtering (30 yr spline) of the individual series; middle panel: RBAR values (calculated for 50 yr windows with 25 yr overlap), mean: 0.26; lower panel: EPS values (50 yr window, 25 yr overlap), mean: 0.89

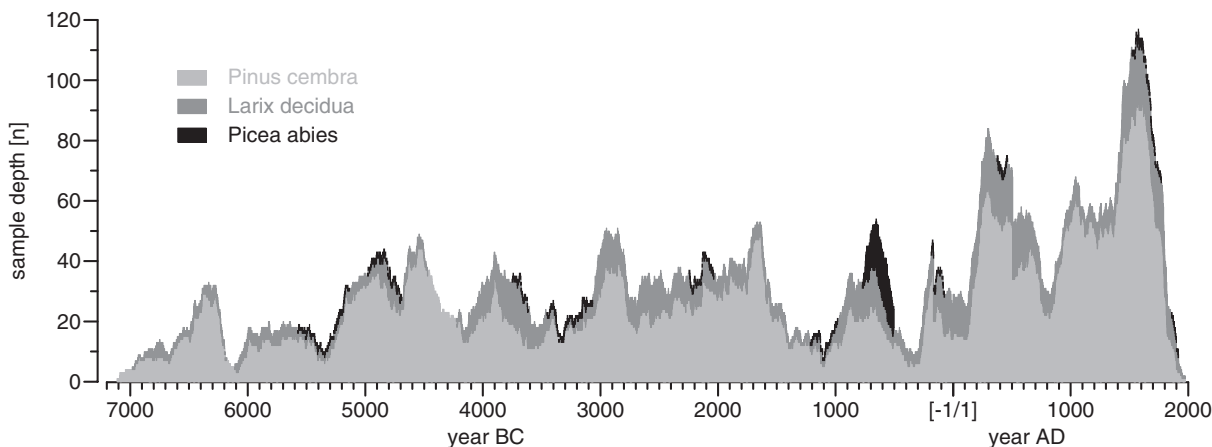


Figure 3 Sample depth of the EACC (excluding tree-ring data from living trees) and the temporal distribution of subfossil/dry-dead samples of the tree species *Pinus cembra* ($n=1167$), *Larix decidua* ($n=237$) and *Picea abies* ($n=28$)

ice-cores (Rasmussen *et al.*, 2007). It may not be accidental that the EACC begins shortly after the 9.3 ka event, another of these events that started around 7300 BC.

As shown, the replication record of the EACC (Figure 3) is triggered by the environmental and climatic evolution in the central Eastern Alps. Therefore, it can be regarded as a low-frequency climatic record. One of the drivers of natural climatic variability is the sun (eg, Bond *et al.*, 2001; Jansen *et al.*, 2007) and records of ^{10}Be have been used as indicator for solar variability in the past (Beer *et al.*, 1988; Bard *et al.*, 1997). Figure 6 shows the comparison of the sample depth record of the EACC with the mid-Holocene ^{10}Be record from the GISP2 ice core (Finkel and Nishiizumi, 1997). The

sample depth record is plotted on a logarithmic scale to highlight minima. The original timescale of the ^{10}Be record is adjusted negatively by 60 years following the suggestions by Southon (2002). The two records show a similar evolution in several parts of their overlap, eg, around 5100 BC and 1600 BC. However, without the shift of the ^{10}Be timescale some of the wiggles, especially those around 3500 BC, would not be in phase.

The significance of the influence of the sun's variations on the Holocene mid-term evolution of the environment and climate in the Alps has been discussed by several authors (eg, Magny, 2004; Holzhauser *et al.*, 2005). These studies demonstrate that periods with reduced solar activity are synchronous with phases of high lake

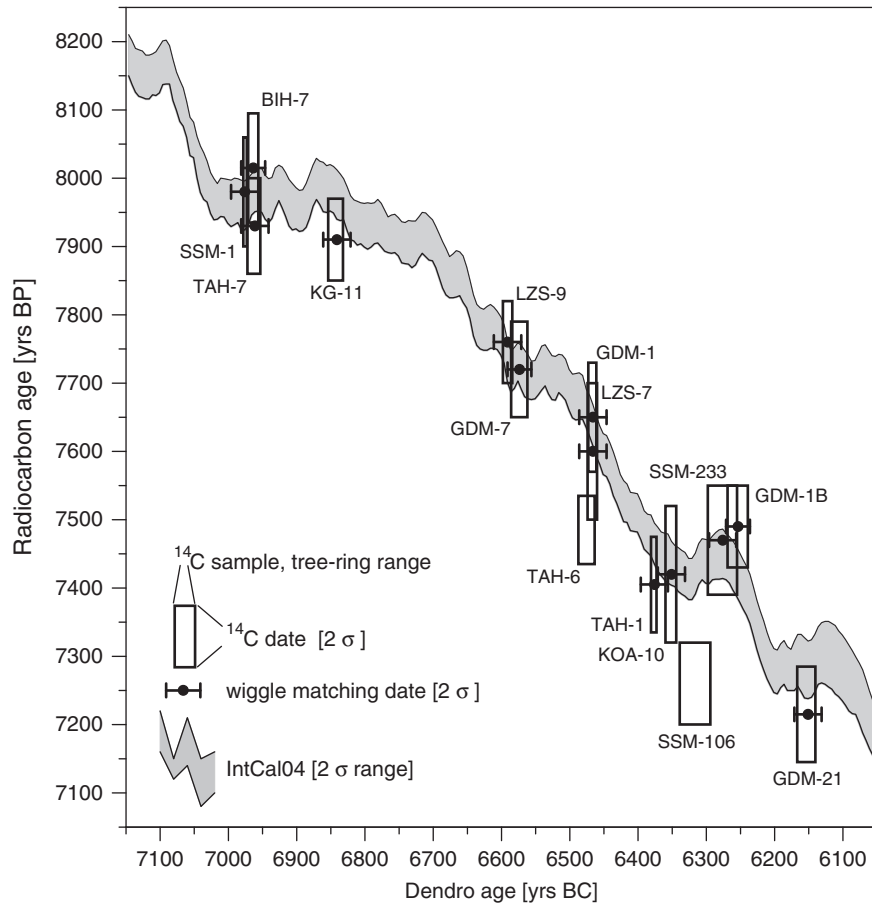


Figure 4 The ¹⁴C-results for the first millennium of the EACC (approx. 7100 to 6100 BC) in relation to the IntCal04 calibration curve (2 σ range). All samples are plotted as rectangles because of the uncalibrated ¹⁴C-date (2 σ range) and the calendar date of the tree-ring sequence analysed. Additionally the wiggle matching results for 13 ¹⁴C-samples are indicated. The error bars indicate the 2 σ range of the result of these combined ¹⁴C dates. Note: the two outlier samples, TAH-6 and SSM-106, were not used for wiggle matching calculation

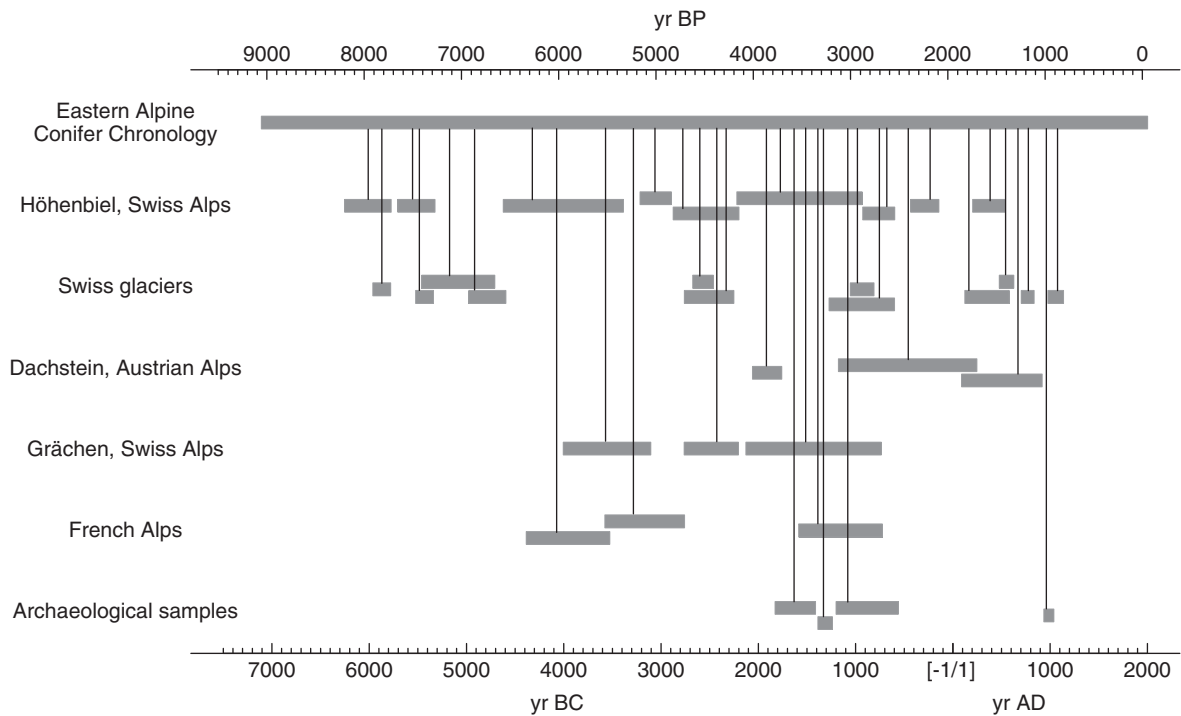


Figure 5 The network of Alpine conifer tree-ring series and chronologies covering the last 9000 years. Calendar dating of previously floating tree-ring series and chronologies is based on the EACC. For references: (a) Renner (1982); Bircher (1982); (b) Renner (1982); Holzhauser (1997); Holzhauser, unpublished data, 2004.; Nicolussi, unpublished data, 2008; (c) Grabner and Gindl (2000); Grabner *et al.* (2001); (d) Schär and Schweingruber (1987, 1988); (e) Edouard *et al.* (2002); (f) Seifert (2000); Reitmaier and Nicolussi (2002); Pichler *et al.* (2009); Nicolussi, unpublished data, 2004

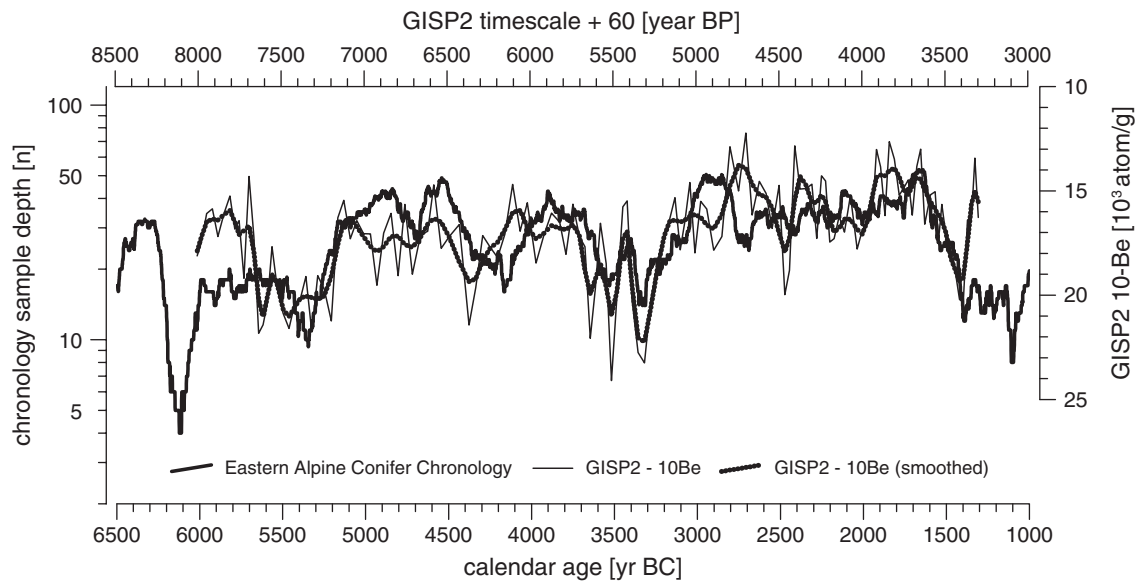


Figure 6 Comparison of the sample depth record of the EACC and the ^{10}Be record of the GISP2 ice core. The ^{10}Be record is shifted backwards by 60 years to the past in relation to the original timescale according to Southon (2002). The ^{10}Be record is also shown smoothed to reduce variability and emphasize the long-term evolution of this data set

levels and glacier advances. Winter (snow) precipitation is one of the important factors that controls glacier variability (eg, Nesje *et al.*, 2008) and it also influences the position of the Alpine treeline. This effect is clearly shown by the regional distribution of treeline altitudes in the Alps (eg, Mayer, 1974). Areas with higher precipitation, eg, at the northern and southern borders of the Alps, show lower treeline positions whereas the central and drier parts display the highest positions of the Alpine treeline, up to approximately 2400 m a.s.l. These observations demonstrate the influence of the length of the vegetation season on tree occurrence due to the duration of the snow cover and the onset of the winter (snow) season at high altitudes. Effects of wetter/cooler climatic conditions due to reduced solar activity (Magny, 2004; Holzhauser *et al.*, 2005) may be an important factor to explain the variations in the sample depth record of the EACC in periods without human impact on the treeline ecotone. Several minima in the sample depth record of the EACC are also synchronous with glacier advance periods, eg, approximately 6200 BC (Kerschner *et al.*, 2006), 4300 BC (Renner, 1982; Nicolussi and Patzelt, 2001), 3600 BC (Patzelt and Bortenschlager, 1973; Nicolussi and Patzelt, 2001) 600 BC and AD 800 (Holzhauser *et al.*, 2005; Nicolussi *et al.*, 2006). Solar activity could have influenced both glacier activity and the treeline position and forest density in the treeline ecotone at least in the mid-Holocene period.

Conclusions

(1) A 9111 yr long tree-ring width chronology has been established based on the analysis of samples from sites above approximately 2000 m a.s.l. mainly in the Eastern Alps.

(2) The establishment of the ultra-long Eastern Alpine Conifer Chronology (EACC) allowed the development of a network of calendar dated Alpine tree-ring chronologies and series. It can be used as a dating base for several research fields in environmental and climatic change in the European Alps as well as for archaeological studies.

(3) The EACC may reflect global as well as regional climatic variability. This is shown by the recording of major North-Hemispheric events, eg, the Tambora 1815 event or the events following major climatic disturbance *c.* AD 540.

(4) The ability to find wooden remains at high altitudes in the Alps before the onset of the Bronze Age displayed in the sample depth record of the EACC seems to be strongly coupled with the forest density and therefore with the climatic history in this mountain area. The accurately dendrochronologically dated early- to mid-Holocene evolution of the treeline ecotone of the central Alps may be partly controlled by solar activity. Human activities in the treeline ecotone as recorded by archaeological findings and pollen analyses may be responsible for the low number of samples found for the Bronze Age (2200–800 BC) and Iron Age (800–15 BC), respectively.

Acknowledgements

We thank Ulrich Jörin, Gerhard Lumassegger, Roland Luzian, Gernot Patzelt, Thomas Pichler and Peter Pindur for their help in the field and/or laboratory. We are grateful to Fritz Schweingruber, Michael Grabner, Hanspeter Holzhauser and Jean-Louis Edouard for the access to unpublished tree-ring data. Brian Luckman and an anonymous reviewer are acknowledged for their comments that helped to improve the clarity of the manuscript. This research has been supported by the Austrian Science Fund (FWF, grants to KN: P13065-GEO, P15828-N06, F3113-G02). TMM acknowledges current support from The Leverhulme Trust (A20060286).

References

- Alley, R.B. and Agustsdottir, A.M. 2005: The 8 k event: cause and consequences of a major Holocene abrupt climate change. *Quaternary Science Reviews* 24, 1123–49.
- Artmann, A. 1949: Jahrringchronologische und -klimatologische Untersuchungen an der Zirbe und anderen Bäumen des Hochgebirges. Unpublished Dissertation University of München, 87 pp.
- Bard, E., Raisbeck, G., Yiou, F. and Jouzel, J. 1997: Solar modulation of cosmogenic nuclide production over the last millennium: comparison between ^{14}C and ^{10}Be records. *Earth and Planetary Science Letters* 150, 453–62.
- Bebber, A.E. 1990: Una cronologia del larice (*Larix decidua* Mill.) delle Alpi orientali italiane. *Dendrochronologia* 8, 119–40.

- Beer, J., Siegenthaler, U., Bonani, G., Finkel, R.C., Oeschger, H., Suter, M. and Wölfli, W. 1988: Information on past solar activity and geomagnetism from ^{10}Be in the Camp Century ice core. *Nature* 331, 675–79.
- Bircher, W. 1982: Zur Gletscher- und Klimageschichte des Saastales. Unpublished Dissertation University of Zürich, 233 pp.
- Bond, G., Kromer, B., Beer, J., Muscheler, R., Evans, M.N., Showers, W., Hoffmann, S., Lotti-Bond, R., Hajdas, I. and Bonani, G. 2001: Persistent solar influence on North Atlantic climate during the Holocene. *Science* 294, 2130–36.
- Bortenschlager, S. 2000: The Iceman's environment. In Bortenschlager, S. and Oeggl, K., editors, *The iceman and his natural environment: palaeobotanical results. The man in the ice, volume 4*. Springer, 11–24.
- Brehme, K. 1951: Jahrringchronologische und -klimatologische Untersuchungen an Hochgebirgslärchen des Berchtesgadener Landes. *Zeitschrift für Weltwirtschaft* 14, 65–80.
- Briffa, K.R., Osborn, T.J., Schweingruber, F.H., Jones, P.D., Shiyatov, S.G. and Vaganov, E.A. 2002: Tree-ring width and density data around the Northern Hemisphere: part 2, spatio-temporal variability and associated climate patterns. *The Holocene* 12, 759–89.
- Bronk Ramsey, C. 1995: Radiocarbon calibration and analysis of stratigraphy: the OxCal program. *Radiocarbon* 37, 425–30.
- 2001: Development of the radiocarbon program OxCal. *Radiocarbon* 43, 355–63.
- Bronk-Ramsey, C., van der Plicht, J. and Weninger, B. 2001: 'Wiggle matching' radiocarbon dates. *Radiocarbon* 43, 381–89.
- Büntgen, U., Esper, J., Frank, D.C., Nicolussi, K. and Schmidhalter, M. 2005: A 1052-year tree-ring proxy for Alpine summer temperatures. *Climate Dynamics* 25, 141–53.
- Cook, E.R. and Peters, K. 1981: The smoothing spline: a new approach to standardizing forest interior tree-ring width series for dendroclimatic studies. *Tree-Ring Bulletin* 41, 45–53.
- D'Arrigo, R., Jacoby, G., Frank, D., Pederson, N., Cook, E., Buckley, B., Nachin, B., Mijiddorj, R. and Dugarjav, C. 2001: 1738 years of Mongolian temperature variability inferred from a tree-ring width chronology of Siberian pine. *Geophysical Research Letters* 28, 543–46.
- Dellinger, F., Kutschera, W., Nicolussi, K., Schießling, P., Steier, P. and Wild, E.M. 2004: A ^{14}C calibration with AMS from 3500 to 3000 BC, derived from a new high-elevation stone-pine tree-ring chronology. *Radiocarbon* 46, 969–78.
- Donati, P., Orcel, A. and Orcel, Ch. 1988: Dendrochronologia e monumenti nell'area ticinese. *Zeitschrift für schweizerische Archäologie und Kunstgeschichte* 45, 277–94.
- Eckstein, D. and Aniol, R.W. 1981: Dendroclimatological reconstruction of the summer temperatures for an alpine region. *Mitteilungen der Forstlichen Bundesversuchsanstalt Wien* 142, 391–98.
- Edouard, J.L., Guibal, F., Nicault, A., Rathgeber, C., Tessier, L., Thomas, A. and Wicha, S. 2002: Arbres subfossiles (*Pinus cembra*, *Pinus uncinata* et *Larix decidua*) et évolution des forêts d'altitude dans les Alpes françaises au cours de l'Holocène. Approche dendrochronologique. In Richard, H. and Vignot, A., editors, *Equilibre et rupture dans les écosystèmes depuis 20000 ans en Europe de l'Ouest*. Colloque international de Besançon, 18–22 septembre 2000. Collection Annales littéraires, Série Environnement, Sociétés et Archéologie, no. 3. Presses Universitaires de Franche-Comté, Les Belles Lettres, 403–11.
- Esper, J., Cook, E.R. and Schweingruber, F.H. 2002: Low-frequency signals in long tree-ring chronologies and the reconstruction of the past temperature variability. *Science* 295, 2250–53.
- Esper, J., Büntgen, U., Frank, D.C., Nievergelt, D., Treydte, K. and Verstege, A. 2006: Multiple tree-ring parameters from Atlas cedar (Morocco) and their climatic signal. In Heinrich, I., editor, *Tree rings in archaeology, climatology and ecology*. *TRACE* 4, 46–55.
- Finkel, R.C. and Nishiizumi, K. 1997: Beryllium 10 concentrations in the Greenland Ice Sheet Project 2 ice core from 3–40 ka. *Journal of Geophysical Research* 102, 26 699–706.
- Furrer, G., Burga, C., Gamper, M., Holzhauser, H. and Maisch, M. 1987: Zur Gletscher-, Vegetations- und Klimageschichte der Schweiz seit der Späteiszeit. *Geographica Helvetica* 42, 61–91.
- Grabner, M. and Gindl, W. 2000: Neue Jahrringchronologien vom Dachstein. In Mandl, F., editor, *Alpen, Archäologie, Felsbildforschung V. Mitteilungen der ANISA* 21, 20–30.
- Grabner, M., Wimmer, R., Gindl, W. and Nicolussi, K. 2001: A 3474-year alpine tree-ring record from the Dachstein, Austria. In Kaennel Dobbertin, M. and Bräker, O.U., editors, *Tree rings and people*. Proceedings of the International Conference on the future of Dendrochronology, 22–26 September 2001, Davos, Switzerland. Swiss Federal Research Institute WSL, 252–53.
- Holzhauser, H. 1997: Fluctuations of the Grosser Aletsch Glacier and the Gorner Glacier during the last 3200 years, new results. In Frenzel, B., editor, *Glacier fluctuations during the Holocene. Paläoklimaforschung/Palaeoclimate Research* 24, 35–58.
- Holzhauser, H., Magny, M. and Zumbühl, H.J. 2005: Glacier and lake-level variations in west-central Europe over the last 3500 years. *The Holocene* 15, 789–801.
- Huber, B. 1941: Aufbau einer mitteleuropäischen Jahrring-Chronologie. *Mitteilungen Hermann Göring Akademie der deutschen Forstwissenschaft* 3, 137–42.
- Jansen, E., Overpeck, J., Briffa, K.R., Duplessy, J.-C., Joos, F., Masson-Delmotte, V., Olago, D., Otto-Bliesner, B., Peltier, W.R., Rahmstorf, S., Ramesh, R., Raynaud, D., Rind, D., Solomina, O., Villalba, R. and Zhang, D. 2007: Palaeoclimate. In Solomon, S., Qin, D., Manning, M., Chen, Z., Marquis, M., Averyt, K.B., Tignor, M. and Miller, H.L., editors, *Climate change 2007: the physical science basis*. Contribution of Working Group I to the Fourth Assessment Report of the Intergovernmental Panel on Climate Change. Cambridge University Press, 433–97.
- Jörin, U.E., Stocker, T.F. and Schlüchter, C. 2006: Multicentury glacier fluctuations in the Swiss Alps during the Holocene. *The Holocene* 16, 697–704.
- Jörin, U.E., Nicolussi, K., Fischer, A., Stocker, T.F. and Schlüchter, C. 2008: Holocene optimum events inferred from subglacial sediments at Tschier Glacier, Eastern Swiss Alps. *Quaternary Science Reviews* 27, 337–50.
- Kaiser, K.F. 1991: Tree-rings in Switzerland and other mountain regions: Late Glacial through Holocene. *Paläoklimaforschung/Palaeoclimate Research* 6, 119–32.
- Kerschner, H., Hertl, A., Gross, G., Ivy-Ochs, S. and Kubik, P.W. 2006: Surface exposure dating of moraines in the Kromer valley (Silvretta Mountains, Austria) – evidence for glacial response to the 8.2 ka event in the Eastern Alps? *The Holocene* 16, 7–15.
- Larsen, L.B., Vinther, B.M., Briffa, K.R., Melvin, T.M., Clausen, H.B., Jones, P.D., Siggaard-Andersen, M.-L., Hammer, C.U., Eronen, M., Grudd, H., Gunnarson, B.E., Hantemirov, R.M., Naurzbaev, M.M. and Nicolussi, K. 2008: New ice core evidence for a volcanic cause of the A.D. 536 dust-veil. *Geophysical Research Letters* 35, L04708, doi:10.1029/2007GL032450.
- Lumasegger, G. 1996: Dendrochronologische Untersuchungen an Zirben (*Pinus cembra*) im Waldgrenzbereich des Radurscheltales, Ötztaler Alpen. Diploma thesis, University of Innsbruck, 90 pp.
- Magny, M. 2004: Holocene climatic variability as reflected by mid-European lake-level fluctuations, and its probable impact on prehistoric human settlements. *Quaternary International* 113, 65–79.
- Mayer, H. 1974: *Wälder des Ostalpenraumes*. Fischer, 344 pp.
- Nesje, A., Dahl, S.O., Thun, T. and Nordli, Ø. 2008: The 'Little Ice Age' glacial expansion in western Scandinavia – summer temperature or winter precipitation? *Climate Dynamics* 30, 789–801.
- Naurzbaev, M.M., Vaganov, E.A., Sidorova, O.V. and Schweingruber, F.H. 2002: Summer temperatures in eastern Taimyr inferred from a 2427-year late-Holocene tree-ring chronology and earlier floating series. *The Holocene* 12, 727–36.
- Nicolussi, K. 1995: Jahrringe und Massenbilanz. Dendroclimatologische Rekonstruktion der Massenbilanzreihe des Hintereisferners bis zum Jahr 1400 mittels *Pinus cembra*-Reihen aus den Ötztaler Alpen, Tirol. *Zeitschrift für Gletscherkunde und Glazialgeologie* 30, 11–52.
- 1999: 10 Jahre Dendrochronologie am Institut für Hochgebirgsforschung. *Institut für Hochgebirgsforschung – Jahresbericht* 1998, 27–46.
- Nicolussi, K. and Patzelt, G. 2000: Discovery of early Holocene wood and peat on the forefield of the Pasterze Glacier, Eastern Alps, Austria. *The Holocene* 10, 191–99.
- 2001: Untersuchungen zur holozänen Gletscherentwicklung von Pasterze und Gepatschferner (Ostalpen). *Zeitschrift für Gletscherkunde und Glazialgeologie* 36, 1–87.

- Nicolussi, K., Bortenschlager, S. and Körner, C.** 1995: Increase in tree-ring width in subalpine *Pinus cembra* from the central Alps that may be CO₂-related. *Trees* 9, 181–89.
- Nicolussi, K., Lumassegger, G., Patzelt, G., Pindur, P. and Schießling, P.** 2004: Aufbau einer holozänen Hochlagen-Jahrring-Chronologie für die zentralen Ostalpen: Möglichkeiten und erste Ergebnisse. In Innsbrucker Geographische Gesellschaft, editor, *Innsbrucker Jahresbericht 2001/2002* 16, 114–36.
- Nicolussi, K., Kaufmann, M., Patzelt, G., van der Plicht, J. and Thurner, A.** 2005: Holocene tree-line variability in the Kauner Valley, Central Eastern Alps, indicated by dendrochronological analysis of living trees and subfossil logs. *Vegetation History and Archaeobotany* 14, 221–34.
- Nicolussi, K., Jörin, U., Kaiser, K.F., Patzelt, G. and Thurner, A.** 2006: Precisely dated glacier fluctuations in the Alps over the last four millennia. In Price, M.F., editor, *Global chance in mountain regions*. Sapiens Publishing, 59–60.
- Patzelt, G.** 1996: Modellstudie Ötztal – Landschaftsgeschichte im Hochgebirgsraum. *Mitteilungen der Österreichischen Geographischen Gesellschaft* 138, 53–70.
- Patzelt, G. and Bortenschlager, S.** 1973: Die postglazialen Gletscher- und Klimaschwankungen in der Venedigergruppe (Hohe Tauern, Ostalpen). *Zeitschrift für Geomorphologie Neues Funde, Supplementen Band* 16, 25–72.
- Pichler, T., Nicolussi, K. and Goldenberg, G.** 2009: Dendrochronological analysis and dating of wooden artefacts from the prehistoric copper mine Kelchalm/Kitzbühel (Austria). *Dendrochronologia* in press.
- Rasmussen, S.O., Vinther, B.M., Clausen, H.B. and Andersen, K.K.** 2007: Early Holocene climate oscillations recorded in three Greenland ice cores. *Quaternary Science Reviews* 26, 1907–14.
- Reimer, P.J., Baillie, M.G.L., Bard, E., Bayliss, A., Beck, J.W., Bertrand, C.J.H., Blackwell, P.G., Buck, C.E., Burr, G.S., Cutler, K.B., Damon, P.E., Edwards, R.L., Fairbanks, R.G., Friedrich, M., Guilderson, T.P., Hogg, A.G., Hughen, K.A., Kromer, B., McCormac, G., Manning, S., Ramsey, C.B., Reimer, R.W., Remmele, S., Southon, J.R., Stuiver, M., Talamo, S., Taylor, F.W., Van Der Plicht, J. and Weyhenmeyer, C.E.** 2004: IntCal04 terrestrial radiocarbon age calibration, 0–26 cal kyr BP. *Radiocarbon* 46, 1029–58.
- Reitmaier, T. and Nicolussi, K.** 2002: Ein hochmittelalterlicher Einbaum aus dem Obersee, Gemeinde St. Jakob/Deferegggen (Osttirol), und die fischereiwirtschaftliche Nutzung alpiner Hochgebirgsseen in Tirol. *NAU – Nachrichtenblatt Arbeitskreis Unterwasserarchäologie* 9, 12–16.
- Renner, F.** 1982: Beiträge zur Gletschergeschichte des Gotthardgebietes und dendroklimatologische Analysen an fossilen Hölzern. Unpublished Dissertation University of Zürich, 180 pp.
- Röthlisberger, F., Haas, P., Holzhauser, H., Keller, W., Bircher, W. and Renner, F.** 1980: Holocene climatic fluctuations – radiocarbon dating of fossil soils (fAh) and woods from moraines and glaciers in the Alps. *Geographica Helvetica* 35, 21–52.
- Schär, E. and Schweingruber, F.H.** 1987: Nacheiszeitliche Stammfunde aus Grächen im Wallis. *Schweizerische Zeitschrift für das Forstwesen* 138, 497–515.
- 1988: 4000 years' forest development in pre-Christian times near a mountain lake in the Alps. *Dendrochronologia* 6, 131–40.
- Schweingruber, F.H.** 1987: Flächenhafte dendroklimatische Temperaturekonstruktionen für Europa. *Naturwissenschaften* 74, 205–12.
- Seifert, M.** 2000: Vor 3466 Jahren erbaut! Die Quellfassung von St. Moritz. *Archäologie der Schweiz* 23, 63–75.
- Southon, J.** 2002: A first step to reconciling the GRIP and GISP2 ice-core chronologies, 0–14,500 yr B.P. *Quaternary Research* 57, 32–37.
- Spurk, M., Leuschner, H.H., Baillie, M.G.L., Briffa, K.R. and Friedrich, M.** 2002: Depositional frequency of German subfossil oaks: climatically and non-climatically induced fluctuations in the Holocene. *The Holocene* 12, 707–15.
- von Grafenstein, U., Erlenkeuser, H., Brauer, A., Jouzel, J. and Johnsen, S.** 1999: A mid-European decadal isotope-climate record from 15,500 to 5,000 years B.P. *Science* 284, 1654–57.
- Wick, L. and Tinner, W.** 1997: Vegetation changes and timberline fluctuations in the Central Alps as indicators of Holocene climatic oscillations. *Arctic and Alpine Research* 29, 445–58.
- Wigley, T.M.L., Briffa, K.R. and Jones, P.D.** 1984: On the average value of correlated time series, with applications in dendroclimatology and hydrometeorology. *Journal of Climate and Applied Meteorology* 23, 201–13.